Transp Porous Med (2011) 86:103–124
DOI 10.1007/s11242-010-9608-6

Effect of Thermal Non-Equilibrium on Convective Instability in a Ferromagnetic Fluid-Saturated Porous Medium

Jinho Lee · I. S. Shivakumara · M. Ravisha

Received: 19 May 2010 / Accepted: 7 June 2010 / Published online: 29 June 2010

Abstract The effect of local thermal non-equilibrium (LTNE) on the onset of thermomagnetic convection in a ferromagnetic fluid-saturated horizontal porous layer in the presence of a uniform vertical magnetic field is investigated. A modified Forchheimer-extended Darcy equation is employed to describe the flow in the porous medium, and a two-field model is used for temperature representing the solid and fluid phases separately. It is found that both the critical Darcy–Rayleigh number and the corresponding wave number are modified by the LTNE effects. Asymptotic solutions for both small and large values of scaled interphase heat transfer coefficient H_t are presented and compared with those computed numerically. An excellent agreement is obtained between the asymptotic and the numerical results. Besides, the influence of magnetic parameters on the instability of the system is also discussed. The available results in the literature are recovered as particular cases from the present study.

Keywords Magnetic fluid · Porous medium · Thermal non-equilibrium model · Thermomagnetic convection

J. Lee · I. S. Shivakumara
School of Mechanical Engineering, Yonsei University, Seoul 120-749, South Korea
e-mail: jinholee@yonsei.ac.kr

I. S. Shivakumara (✉)
Department of Mathematics, UGC-Centre for Advanced Studies in Fluid Mechanics, Bangalore University, Bangalore 560001, India
e-mail: shivakumarais@gmail.com

M. Ravisha
Department of Mathematics, Smt. Rukmini Shedthi Memorial National Government First Grade College, Udupi District, Barkur 576210, India
e-mail: ravishmamatha@gmail.com

List of Symbols

$a = \sqrt{\ell^2 + m^2}$	Overall horizontal wavenumber
$\vec{B}$	Magnetic induction
c	Specific heat
c_{F}	Dimensionless form drag constant
d	Thickness of the porous layer
$D = \mathrm{d}/\mathrm{d}z$	Differential operator
$\vec{g}$	Acceleration due to gravity
h	Heat transfer coefficient
$\vec{H}$	Magnetic field intensity
H_0	Imposed uniform vertical magnetic field
$H_{\mathrm{t}} = hd^2/\varepsilon k_{\mathrm{tf}}$	Scaled inter-phase heat transfer coefficient
$\hat{k}$	Unit vector in z-direction
k	Permeability of the porous medium
k_{t}	Thermal conductivity
$K = -(\partial M/\partial T)_{H_0,T_0}$	Pyromagnetic co-efficient
ℓ, m	Wave numbers in the x and y directions
$\vec{M}$	Magnetization
$M_0 = M(H_0, T_0)$	Constant mean value of magnetization
$M_1 = \mu_0 K^2 \beta/(1+\chi)\alpha_{\mathrm{t}}\rho_0 g$	Magnetic number
$M_3 = (1 + M_0/H_0)/(1+\chi)$	Non-linearity of magnetization parameter
p	Pressure
$\vec{q} = (u, v, w)$	Velocity vector
$R = \rho_0 \alpha_{\mathrm{t}} g \beta k d^2/\varepsilon \mu_f \kappa_{\mathrm{f}}$	Darcy–Rayleigh number
$R_{\mathrm{m}} = RM_1$	Magnetic Darcy–Rayleigh number
t	Time
T	Temperature
T_{l}	Temperature of the lower boundary
T_{u}	Temperature of the upper boundary
$T_{\mathrm{a}} = (T_{\mathrm{l}} + T_{\mathrm{u}})/2$	Reference temperature
W	Amplitude of vertical component of perturbed velocity
(x, y, z)	Cartesian co-ordinates

Greek Symbols

α_{t}	Thermal expansion coefficient
$\beta = \Delta T/d$	Temperature gradient
$\chi = (\partial M/\partial H)_{H_0,T_0}$	Magnetic susceptibility
$\nabla^2 = \partial^2/\partial x^2 + \partial^2/\partial y^2 + \partial^2/\partial z^2$	Laplacian operator
$\nabla_{\mathrm{h}}^2 = \partial^2/\partial x^2 + \partial^2/\partial y^2$	Horizontal Laplacian operator
ε	Porosity of the porous medium
$\kappa_{\mathrm{f}} = k_{\mathrm{tf}}/(\rho_0 c)_f$	Thermal diffusivity of the fluid
μ_{f}	Dynamic viscosity
μ_0	Free space magnetic permeability of vacuum
φ	Magnetic potential
Φ	Amplitude of perturbed magnetic potential
$\gamma = \varepsilon k_{\mathrm{tf}}/(1-\varepsilon)k_{\mathrm{ts}}$	Porosity modified conductivity ratio
ρ_{f}	Fluid density

ρ_0 Reference density at T_a
Θ Amplitude of temperature

Subscripts

b Basic state
f Fluid
s Solid

1 Introduction

Ferrofluids or magnetic fluids are colloidal suspensions of magnetic nanoparticles in a carrier fluid such as water, hydrocarbon (mineral oil or kerosene), or fluorocarbon. The nanoparticles typically have sizes of about 10 nm and they are coated with surfactants to prevent the coagulation. These fluids are also referred to as magnetic nanofluids which are unique materials having both the liquid and magnetic properties. Ferrofluids are not naturally occurring but they are synthesized in the laboratory. These fluids can be easily manipulated with an external magnetic field, and hence they are exciting system from fundamental and application points of view (Rosensweig 1985; Berkovsky et al. 1993; Blums et al. 1997; Hergt et al. 1998; Alexiou et al. 2001). Mechanical engineering industries use them as fluids in vibration dampers, shock absorbers, and vacuum seals. Electrical and electronic industries use ferrofluids to improve hi-fi characteristic loud speakers, as transformer coolants and also in miniaturizing inductive components. Computation industries use them as fluids in stepper motors. Therefore, studies on ferrofluids have received much attention in the scientific community over the years

The magnetization of ferrofluids depends on the magnetic field, temperature, and density. Hence, any variations of these quantities induce change of body force distribution in the fluid and eventually give rise to convection in ferrofluids in the presence of a gradient of magnetic field. Of late, researchers are looking for new technologies to improve the operation of existing oil-cooled electromagnetic equipment. One of the approaches suggested in the literature is to replace the oil in such devices with oil-based ferrofluids, which can take advantage of the pre-existing leakage magnetic fields to enhance heat transfer processes. Hence the study of thermal convection in magnetized ferrofluids has triggered lot of research interest on this topic considering the prospect of heat transfer applications in electronics, engines, and micro and nanoelectromechanical systems. There have been numerous studies carried out on thermal convection in a ferrofluid layer heated from below called ferroconvection analogous to Rayleigh–Benard convection in ordinary viscous fluids. Finlayson (1970) was the first to study convective instability of a magnetic fluid layer heated from below in the presence of a uniform vertical magnetic field. A linear stability analysis has been carried out to predict the critical gradient of temperature corresponding to the onset of convection when both buoyancy and magnetic forces are included by considering the bounding surfaces of the magnetic fluid layer to be either shear free or rigid. In his review article, Odenbach (2004) has focused on recent developments in the field of rheological investigations of ferrofluids and their importance for the general treatment of ferrofluids. Sunil and Mahajan (2008) have performed nonlinear stability analysis for a magnetized ferrofluid layer heated from below by considering the bounding surfaces are stress-free, while Nanjundappa and Shivakumara (2008) have made a detailed study by considering variety of velocity and temperature boundary conditions on the onset of ferroconvection in an initially quiescent ferrofluid layer. Matura and Lucke (2009) have investigated the influence of time periodic and spatially homogeneous magnetic field on the linear and nonlinear stability of a ferrofluid layer heated from above and below. Thermal convection of ferrofluids in the presence of a uniform vertical magnetic field, with the boundary temperatures modulated sinusoidally about some reference values, has been studied by Singh and Bajaj (2009) with the idea of understanding control of ferroconvection. Recently, Nanjundappa et al. (2010) have investigated theoretically the effect of magnetic field dependent viscosity on the onset of Benard–Marangoni ferroconvection in a horizontal layer of ferrofluid.

Thermal convection of ferrofluids saturating a porous medium has also attracted considerable attention in the literature owing to its importance in controlled emplacement of liquids or treatment of chemicals, and emplacement of geophysically imageble liquids into particular zones for subsequent imaging, etc. Rosensweig et al. (1978) have studied experimentally the penetration of ferrofluids in the Hele–Shaw cell. The stability of the magnetic fluid penetration through a porous medium in high uniform magnetic field oblique to the interface is studied by Zhan and Rosensweig (1980). The thermal convection of ferrofluid saturating a porous medium in the presence of a vertical magnetic field is studied by Vaidaynathan et al. (1991) by employing the Brinkman equation. Qin and Chadam (1995) have carried out the non-linear stability analysis of ferroconvection in a porous layer by including the inertial effects to accommodate high velocity. The laboratory scale experimental results of the behavior of ferrofluids in porous media consisting of sands and sediments are presented by Borglin et al. (2000). Sunil and Mahajan (2009) have used generalized energy method to study nonlinear convection in a magnetized ferrofluid-saturated porous layer heated uniformly from below for the stress-free boundaries case. Recently, Shivakumara et al. (2008, 2009) have investigated theoretically the onset of convection in a layer of ferrofluid-saturated porous medium for various types of velocity and temperature boundary conditions.

In many practical applications involving hyper-porous materials and also media in which there is a large temperature difference between the fluid and solid phases, it has been realized that the assumption of local thermal equilibrium (LTE) is inadequate for proper understanding of the heat transfer problems. In such circumstances, the local thermal non-equilibrium (LTNE) effects are to be taken into consideration. Therefore, the recent trend in the study of thermal convective instability problems in porous media is to account for LTNE effects by considering a two-field model for energy equation each representing the fluid and solid phases separately. Realizing this fact, investigations have been carried out in the recent past to know LTNE effects on forced and free convection in porous media involving ordinary viscous fluids. The LTNE effects on forced convection flows in a porous medium have been covered exhaustively in the excellent reviews by Vafai and Amiri (1998) and Kuznetsov (1998). Rees and Pop (1999, 2000, 2002), Banu and Rees (2002), and Postelnicu and Rees (2003) have investigated LTNE effect on free convective flows in a porous medium. Rees and Pop (2005) have reviewed the works on LTNE phenomena in a porous medium convection, primarily free and forced convection boundary layers and free convection within cavities. The effect of LTNE on the onset of convection in a porous layer has been studied using a non-Darcian model for stress-free boundaries by Malashetty et al. (2005a) and with an additional effect of anisotropy in permeability as well as thermal diffusivity by Malashetty et al. (2005b). Straughan (2006) has considered a problem of thermal convection in a fluid-saturated porous layer using a global nonlinear stability analysis with a LTNE model. Malashetty et al. (2006) and Shivakumara et al. (2006) have analyzed the onset of convection in a porous layer saturated with an

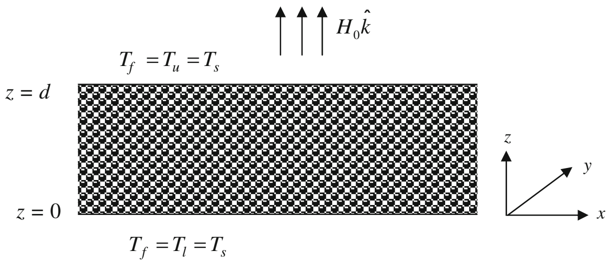

Fig. 1 Physical configuration

Oldroyd-B fluid by considering a LTNE model. Nouri–Borujerdi et al. (2007a) have discussed the effect of internal heat generation and thermal non-equilibrium effects on the onset of convection in a porous channel. In a subsequent paper, Nouri-Borujerdi et al. (2007b) have analyzed the effect of thermal non-equilibrium on impulsive conduction in porous media. Postelnicu (2008) has studied the onset of Darcy–Brinkman convection using a thermal non-equilibrium model for rigid isothermal boundaries. Recently, Shivakumara et al. (2010a,b)have analyzed the effects of temperature dependent viscosity and quadratic density as well as boundary effect on the onset of free convection in a porous layer using a thermal non-equilibrium model.

Nonetheless, the studies on thermomagnetic convection in a ferromagnetic fluid-saturated porous medium are based only on LTE model, and no attention has been given to assess LTNE effects on the criterion for the onset of ferroconvection despite its relevance and importance in many heat transfer problems as noted above. The novelty of the present study is to investigate how the onset criterion for thermomagnetic convection in a horizontal ferromagnetic fluid-saturated porous layer is affected by the adoption of LTNE model. In analyzing the problem, a two-field model for the separate modeling of the solid and fluid phase temperature fields in a ferromagnetic fluid-saturated porous medium is used and the flow in the porous medium is described by the modified Forchheimer-extended Darcy equation. The bounding surfaces of the porous layer are considered to be impermeable, ferromagnetic, and perfect thermal conductors. The criterion for the onset of convection is analyzed analytically, and the existing results are obtained as particular cases from the present study. It is observed that the form-drag has no influence on the stability criteria since the basic state whose stability is being analyzed is quiescent.

2 Formulation of the Problem

We consider an initially quiescent incompressible constant viscosity ferromagnetic fluid-saturated horizontal porous layer of characteristic thickness d in the presence of a uniform applied magnetic field H_0 in the vertical direction as shown in Fig. 1. The lower surface is held at constant temperature T_l, while the upper surface is at $T_\mathrm{u} (< T_\mathrm{l})$. A Cartesian co-ordinate system (x, y, z) is used with the origin at the bottom of the porous layer and the z-axis directed vertically upward in the presence of gravitational field. The solid and fluid phases of the porous medium are assumed to be in LTNE, and a two-field model for temperatures is used (Nield and Bejan 2006).

The basic equations governing the flow of an incompressible ferrofluid saturating a porous medium are given as follows:

The continuity equation is

$$\nabla \cdot \vec{q} = 0, \tag{1}$$

where $\vec{q}$ is the velocity vector.

The momentum equation is

$$\frac{\rho_0}{\varepsilon}\frac{\partial \vec{q}}{\partial t} = -\nabla \mathrm{p} + \rho_{\mathrm{f}}\vec{g} - \frac{\mu_{\mathrm{f}}}{k}\vec{q} - \frac{\rho_0 c_{\mathrm{F}}}{\sqrt{k}}\,|\vec{q}|\,\vec{q} + \mu_0(\vec{M}\cdot\nabla)\vec{H}, \tag{2}$$

where p the pressure, $\vec{M}$ the magnetization, $\vec{H}$ the magnetic field intensity, ρ_{f} the fluid density, k the permeability of the porous medium, c_{F} the dimensionless form drag constant, ε the porosity of the porous medium, μ_{f} the fluid viscosity, μ_0 the magnetic permeability of vacuum and $\nabla^2 = \partial^2/\partial x^2 + \partial^2/\partial y^2 + \partial^2/\partial z^2$ is the Laplacian operator. The term $\mu_0(\vec{M}\cdot\nabla)\vec{H}$ in the above equation is the magnetic body force which appears as a result of polarization of the ferrofluid in the presence of magnetic field.

The temperature equation for the fluid and solid phases are, respectively, given by

$$\varepsilon\,(\rho_0 c)_{\mathrm{f}}\frac{\partial T_{\mathrm{f}}}{\partial t} + (\rho_0 c)_{\mathrm{f}}\,(\vec{q}\cdot\nabla)\,T_{\mathrm{f}} = \varepsilon k_{\mathrm{tf}}\nabla^2 T_{\mathrm{f}} + h\,(T_{\mathrm{s}} - T_{\mathrm{f}}) \tag{3}$$

$$(1-\varepsilon)\,(\rho_0 c)_{\mathrm{s}}\frac{\partial T_{\mathrm{s}}}{\partial t} = (1-\varepsilon)\,k_{\mathrm{ts}}\nabla^2 T_{\mathrm{s}} - h\,(T_{\mathrm{s}} - T_{\mathrm{f}})\,, \tag{4}$$

where T the temperature, c the specific heat, k_{t} the thermal conductivity, and h is the interphase heat transfer coefficient which depends on the nature of the porous matrix and the saturating ferrofluid. It may be noted that large values of h correspond to a rapid transfer of heat between the phases which represents the LTE case, while moderate values of h gives raise to relatively strong LTNE effects. In other words, it measures the ease with which heat is transferred between the phases. The subscripts f and s represent the fluid and solid phases, respectively.

The fluid density is assumed to vary in the form

$$\rho_{\mathrm{f}} = \rho_0\left[1 - \alpha_{\mathrm{t}}\,(T_{\mathrm{f}} - T_{\mathrm{a}})\right], \tag{5}$$

where ρ_0 is the reference value, α_{t} is the thermal expansion coefficient and $T_{\mathrm{a}} = (T_{\mathrm{l}} + T_{\mathrm{u}})\,/2$ is the average temperature.

The Maxwell equations in the magnetostatic limit are:

$$\nabla \cdot \vec{B} = 0 \tag{6a}$$

$$\nabla \times \vec{H} = 0 \text{ or } \vec{H} = \nabla\varphi, \tag{6b}$$

where $\vec{B}$ is the magnetic induction and φ is the magnetic potential.

Further, $\vec{B}$, $\vec{M}$, and $\vec{H}$ are related by

$$\vec{B} = \mu_0(\vec{M} + \vec{H}). \tag{7}$$

It is assumed that the magnetization is aligned with the magnetic field, but allowed a dependence on the magnitude of the magnetic field as well as temperature (Finlayson 1970) and thus

$$\vec{M} = M(H, T_{\mathrm{f}})\frac{\vec{H}}{H}, \tag{8}$$

where $M = \left|\vec{M}\right|$ and $H = \left|\vec{H}\right|$. The magnetic equation of state, following (Finlayson 1970), is taken as

$$M = M_0 \; + \; \chi(H - H_0) \; - \; K(T_{\mathrm{f}} - T_{\mathrm{a}}), \tag{9}$$

where $\chi = (\partial M/\partial H)_{H_0,T_a}$ is the magnetic susceptibility, $K = -(\partial M/\partial T_f)_{H_0,T_a}$ is the pyromagnetic co-efficient, and $M_0 = M(H_0, T_a)$.

The basic state is quiescent and there exists the following solution for the basic state:

$$\begin{aligned}
&\vec{q}_{\mathrm{b}} = 0\\
&p_{\mathrm{b}}(z) = p_0 - \rho_0 g z - \frac{1}{2}\rho_0 \alpha_t g \beta z\,(z-d) - \frac{\mu_0 M_0 K\beta}{1+\chi} z - \frac{\mu_0 K^2\beta^2}{2(1+\chi)^2} z\,(z-d)\\
&T_{\mathrm{fb}}(z) = T_{\mathrm{a}} - \beta\,(z - d/2) = T_{\mathrm{sb}}(z)\\
&\vec{H}_{\mathrm{b}}\,(z) = \left[H_0 - \frac{K\beta}{1+\chi}\left(z - \frac{d}{2}\right)\right]\hat{k}\\
&\vec{M}_{\mathrm{b}}\,(z) = \left[M_0 + \frac{K\beta}{1+\chi}\left(z - \frac{d}{2}\right)\right]\hat{k},
\end{aligned} \tag{10}$$

where $\beta = \Delta T/d = (T_{\mathrm{l}} - T_{\mathrm{u}})/d$ is the temperature gradient, $\hat{k}$ is the unit vector in the z-direction, and the subscript b denotes the basic state. It may be noted that the fluid and solid phases have the same temperatures at the bounding surfaces of the porous layer.

3 Linear Stability Theory

In order to investigate the conditions under which the quiescent solution is stable against small disturbances, we consider a perturbed state in the form

$$\begin{aligned}
&\vec{q} = \vec{q}\,', \quad p = p_{\mathrm{b}}(z) + p', \quad T_{\mathrm{f}} = T_{\mathrm{fb}}(z) + T_{\mathrm{f}}', \quad T_{\mathrm{s}} = T_{\mathrm{sb}}(z) + T_{\mathrm{s}}',\\
&\vec{H} = \vec{H}_{\mathrm{b}}(z) + \vec{H}', \quad \vec{M} = \vec{M}_{\mathrm{b}}(z) + \vec{M}',
\end{aligned} \tag{11}$$

where $\vec{\mathrm{q}}' = (\mathrm{u}', \mathrm{v}', \mathrm{w}')$, p', T_{f}', T_{s}', $\vec{\mathrm{H}}' = (\mathrm{H}_x', \mathrm{H}_y', \mathrm{H}_z')$ and $\mathrm{M}' = (\mathrm{M}_x', \mathrm{M}_y', \mathrm{M}_z')$ are perturbed variables and are assumed to be small.

Substituting Eq. 11 into Eqs. 7 and 8, and using Eq. 6, we obtain (after dropping the primes)

$$\begin{aligned}
H_x + M_x &= (1 + M_0/H_0)\,H_x\\
H_y + M_y &= (1 + M_0/H_0)\,H_y\\
H_z + M_z &= (1 + \chi)\,H_z - K T_{\mathrm{f}}.
\end{aligned} \tag{12}$$

Again substituting Eq. 11 into momentum Eq. 2, linearizing, eliminating the pressure term by taking curl twice, and using Eq. 12, the z-component of the resulting equation can be obtained as (after dropping the primes):

$$\left[\rho_0\frac{\partial}{\partial t} + \frac{\mu_{\mathrm{f}}}{k}\right]\nabla^2 w = -\mu_0 K\beta\frac{\partial}{\partial z}\left(\nabla_{\mathrm{h}}^2\varphi\right) + \frac{\mu_0 K^2\beta}{1+\chi}\nabla_{\mathrm{h}}^2 T_{\mathrm{f}} + \rho_0\alpha_{\mathrm{t}} g\nabla_{\mathrm{h}}^2 T_{\mathrm{f}}, \tag{13}$$

where $\nabla_{\mathrm{h}}^2 = \partial^2/\partial x^2 + \partial^2/\partial y^2$ is the horizontal Laplacian operator.

Equations 3 and 4, after using Eq. 11 and linearizing, take the following form (after dropping the primes):

$$\varepsilon\,(\rho_0 c)_{\mathrm{f}}\,\frac{\partial T_{\mathrm{f}}}{\partial t}+(\rho_0 c)_{\mathrm{f}}\,w\,\frac{dT_{\mathrm{fb}}}{dz}=\varepsilon k_{\mathrm{tf}}\nabla^2 T_{\mathrm{f}}+h\,(T_{\mathrm{s}}-T_{\mathrm{f}}) \tag{14}$$

$$(1-\varepsilon)\,(\rho_0 c)_{\mathrm{s}}\,\frac{\partial T_{\mathrm{s}}}{\partial t}=(1-\varepsilon)\,k_{\mathrm{ts}}\nabla^2 T_{\mathrm{s}}-h\,(T_{\mathrm{s}}-T_{\mathrm{f}})\,. \tag{15}$$

Equations 6a and 6b, after substituting Eq. 11 and using Eq. 12, may be written as (after dropping the primes)

$$\left(1+\frac{M_0}{H_0}\right)\,\nabla_{\mathrm{h}}^2\varphi+(1+\chi)\,\frac{\partial^2\varphi}{\partial z^2}-K\,\frac{\partial T_{\mathrm{f}}}{\partial z}=0. \tag{16}$$

The principle of exchange of stability is shown to be valid in the cases of (i) ferroconvection in a porous layer without LTNE effect (Shivakumara et al. 2008) and (ii) thermal convection in an ordinary viscous fluid saturating a porous layer with LTNE effect (Malashetty et al. 2005a). Therefore, it is obvious to presume that the principle of exchange of stability is valid for the present setup as well. Accordingly, the normal mode expansion of the dependent variables is assumed in the form

$$\{w,T_{\mathrm{f}},T_{\mathrm{s}},\varphi\}=\{W(z),\Theta_{\mathrm{f}}(z),\Theta_{\mathrm{s}}(z),\Phi(z)\}\exp\left[i\,(\ell x+my)\right], \tag{17a}$$

where ℓ and m are wave numbers in the x and y directions, respectively, $W(z)$ is the amplitude of vertical component of perturbed velocity, $\Theta_{\mathrm{f}}(z)$ is the amplitude of perturbed fluid temperature, $\Theta_{\mathrm{s}}(z)$ is the amplitude of perturbed solid temperature, and $\Phi(z)$ is the amplitude of perturbed magnetic potential.

Substituting Eq. 17a into Eqs. 13–16, and non-dimensionalizing the variables by setting

$$\left(x^*,y^*,z^*\right)=\left(\frac{x^*}{d},\frac{y^*}{d},\frac{z^*}{d}\right),\quad t^*=\frac{\kappa_{\mathrm{f}}}{d^2}t,\quad W^*=\frac{d}{\varepsilon\kappa_{\mathrm{f}}}W,$$
$$\Theta_{\mathrm{f}}^*=\frac{1}{\beta d}\Theta_{\mathrm{f}},\quad \Theta_{\mathrm{s}}^*=\frac{1}{\beta d}\Theta_{\mathrm{s}},\quad \Phi^*=\frac{(1+\chi)}{K\beta d^2}\Phi, \tag{17b}$$

where $\kappa_{\mathrm{f}}=k_{\mathrm{tf}}/(\rho_0 c)_{\mathrm{f}}$ is the effective thermal diffusivity of the fluid, we obtain (after dropping the asterisks for simplicity)

$$\left(D^2-a^2\right)W=a^2R\left[M_1 D\Phi-(1+M_1)\,\Theta_{\mathrm{f}}\right] \tag{18}$$

$$\left(D^2-a^2\right)\Theta_{\mathrm{f}}+H_{\mathrm{t}}\,(\Theta_{\mathrm{s}}-\Theta_{\mathrm{f}})=-W \tag{19}$$

$$\left(D^2-a^2\right)\Theta_{\mathrm{s}}+\gamma H_{\mathrm{t}}\,(\Theta_{\mathrm{f}}-\Theta_{\mathrm{s}})=0 \tag{20}$$

$$\left(D^2-a^2M_3\right)\Phi-D\Theta_{\mathrm{f}}=0. \tag{21}$$

Here, $D=\mathrm{d}/\mathrm{d}z$ is the differential operator, $a=\sqrt{\ell^2+m^2}$ is the overall horizontal wave number, $R=\rho_0\alpha_{\mathrm{t}}g\beta kd^2/\varepsilon\mu_{\mathrm{f}}\kappa_{\mathrm{f}}$ is the Darcy–Rayleigh number and it is a ratio of buoyant to viscous forces, $M_1=\mu_0K^2\beta/(1+\chi)\alpha_{\mathrm{t}}\rho_0 g$ is the magnetic number and it is a ratio of magnetic to gravitational forces, $M_3=(1+M_0/H_0)/(1+\chi)$ is the measure of nonlinearity of magnetization, $H_{\mathrm{t}}=hd^2/\varepsilon k_{\mathrm{tf}}$ is the scaled inter-phase heat transfer coefficient, and $\gamma=\varepsilon k_{\mathrm{tf}}/(1-\varepsilon)\,k_{\mathrm{ts}}$ is the porosity modified conductivity ratio.

Equations 18–21 are to be solved subject to appropriate boundary conditions. The boundaries are impermeable, ferromagnetic, and perfect thermal conductors. The boundary conditions are:

$$W=\Theta_{\mathrm{f}}=\Theta_{\mathrm{s}}=D\Phi=0\quad\text{at } z=0,1. \tag{22}$$

Equations 18–21 admit solutions in the form

$$W = A_1 \sin \pi z, \quad \Theta_f = A_2 \sin \pi z, \quad \Theta_s = A_3 \sin \pi z, \quad \Phi = A_4 \cos \pi z, \tag{23}$$

where $A_1 - A_4$ are constants. Substitution of Eq. 23 into Eqs. 18–21 and eliminating the constants $A_1 - A_4$ from the resulting equations yields the following characteristic equation:

$$\begin{vmatrix} (\pi^2 + a^2) & -a^2 R (1 + M_1) & 0 & -\pi a^2 R M_1 \\ -1 & (\pi^2 + a^2 + H_t) & -H_t & 0 \\ 0 & -\gamma H_t & (\pi^2 + a^2 + \gamma H_t) & 0 \\ 0 & \pi & 0 & (\pi^2 + M_3 a^2) \end{vmatrix} = 0. \tag{24}$$

Expanding the above determinant yields the following expression for the Rayleigh number R:

$$R = \frac{(\pi^2 + a^2)^2 \{\pi^2 + a^2 + H_t (1 + \gamma)\}}{a^2 (\pi^2 + a^2 + \gamma H_t)} \frac{(\pi^2 + M_3 a^2)}{\{\pi^2 + M_3 (1 + M_1) a^2\}}. \tag{25}$$

We note that R attains its critical value R_c at $a^2 = a_c^2$, where a_c^2 satisfies the equation

$$b_1 (a_c^2)^6 + b_2 (a_c^2)^5 + b_3 (a_c^2)^4 + b_4 (a_c^2)^3 + b_5 (a_c^2)^2 + b_6 (a_c^2) + b_7 = 0, \tag{26}$$

where

$$\begin{aligned}
b_1 &= (1 + M_1) M_3^2 \\
b_2 &= 2M_3 \left\{(1 + M_3 + M_1 M_3) \pi^2 + H_t (1 + M_1) M_3 \gamma\right\} \\
b_3 &= \{1 - 2(-2 + M_1) M_3\} \pi^4 + H_t^2 (1 + M_1) M_3^2 \gamma (1 + \gamma) \\
&\quad + H_t M_3 \pi^2 \{-M_3 + 4\gamma + 2M_3\gamma + M_1 (-1 - M_3 + 2M_3\gamma)\} \\
b_4 &= -2\pi^2 \Big[\left\{-1 + M_3^2 + M_1 M_3 (3 + M_3)\right\} \pi^4 - H_t^2 M_3 \gamma (1 + \gamma) \\
&\quad + H_t \pi^2 \left\{-\gamma + (1 + M_1) M_3^2 (1 + \gamma) + M_3 (1 - 2\gamma + 2M_1 (1 + \gamma))\right\}\Big] \\
b_5 &= -\pi^4 \Big[M_3 \{4 + M_3 + M_1 (6 + M_3)\} \pi^4 + H_t^2 \left\{-1 + M_3^2 + M_1 M_3 (2 + M_3)\right\} \gamma (1 + \gamma) \\
&\quad + H_t \pi^2 \left\{1 - 2\gamma + (1 + M_1) M_3^2 (1 + 2\gamma) + M_3 (4 + 5M_1 + 4\gamma + 8M_1\gamma)\right\}\Big] \\
b_6 &= -2\pi^6 \left(H_t + \pi^2 + H_t\gamma\right) \left\{(1 + M_3 + M_1 M_3) \pi^2 + H_t (1 + M_1) M_3 \gamma\right\} \\
b_7 &= -\pi^8 \left\{\pi^4 + H_t^2 \gamma (1 + \gamma) + H_t \pi^2 (1 + 2\gamma)\right\}.
\end{aligned}$$

Equation 26 is solved numerically for various values of M_1, M_3, γ, and H_t and the critical value of a_c^2 is obtained. Using this a_c^2 in Eq. 25, the critical Rayleigh number R_c is obtained, above which the ferroconvection sets in.

It is interesting to check Eq. 25 under some limiting cases. We note that for an ordinary viscous fluid case (i.e., $M_1 = 0$), or when $M_3 = 0$, Eq. 25 reduces to

$$R = \frac{(\pi^2 + a^2)^2 \{\pi^2 + a^2 + H_t (1 + \gamma)\}}{a^2 (\pi^2 + a^2 + \gamma H_t)}. \tag{27}$$

The above expression is the same as the one obtained by Banu and Rees (2002). The value of R given in Eq. 27 attains its critical value R_c at $a^2 = a_c^2$, where a_c^2 satisfies the equation

$$\left(a_c^2\right)^4 + 2\left(\pi^2 + \gamma H_t\right)\left(a_c^2\right)^3 + H\left(\gamma H_t + \gamma^2 H_t - \pi^2 + 2\gamma\pi^2\right)\left(a_c^2\right)^2 \\ -2\pi^4\left(H_t + \pi^2 + \gamma H_t\right)\left(a_c^2\right) - \pi^4\left(\pi^4 + H_t^2\gamma + H_t^2\gamma^2 + H_t\pi^2 + 2\gamma H_t\pi^2\right) = 0. \tag{28}$$

When $H_t = 0$ (LTE case), Eq. 25 reduces to

$$R = \frac{\left(\pi^2 + a^2\right)^2}{a^2} \frac{\left(\pi^2 + M_3 a^2\right)}{\left\{\pi^2 + M_3\left(1 + M_1\right)a^2\right\}}. \tag{29}$$

Equation 29 coincides with the one given by Shivakumara et al. (2008) when $\Lambda = 0$ in their expression for the Rayleigh number.

Further, when $H_t \to \infty$, Eq. 25 reduces to

$$R\left(\frac{\gamma}{1+\gamma}\right) = \frac{\rho_0\alpha_t g\beta k d^2}{\left\{\varepsilon\kappa_f + (1-\varepsilon)\kappa_s\right\}\mu} = \frac{\left(\pi^2 + a^2\right)^2}{a^2} \frac{\left(\pi^2 + M_3 a^2\right)}{\left\{\pi^2 + M_3\left(1 + M_1\right)a^2\right\}}. \tag{30}$$

Here, it is noted that the expression for the Rayleigh number is based on the mean properties of the porous medium and coincides for the LTE case. For the LTE case, R attains its critical value at $a^2 = a_c^2$, where a_c^2 satisfies the equation

$$M_3^2\left(1 + M_1\right)\left(a_c^2\right)^4 + 2\pi^2 M_3\left(a_c^2\right)^3 - \pi^4\left\{M_3^2 + M_1 M_3\left(M_3 + 2\right) - 1\right\}\left(a_c^2\right)^2 \\ -2\pi^6 M_3\left(1 + M_1\right)\left(a_c^2\right) - \pi^8 = 0. \tag{31}$$

When $M_1 = 0 = H_t$, Eq. 25 simply reduces to

$$R = \frac{\left(\pi^2 + a^2\right)^2}{a^2}. \tag{32}$$

Evidently, R given by Eq. 32 attains its minimum when $a = \pi$. That is, the critical Darcy–Rayleigh number is $4\pi^2$ and the associated critical wave number is π; the known results for the classical Darcy–Benard problem.

For very large M_1, the results for the magnetic mechanism alone operating in the absence of buoyancy effects is obtained. The corresponding magnetic Darcy–Rayleigh number $R_m (= RM_1)$ is expressed as follows:

$$R_m = RM_1 = \frac{\left(\pi^2 + a^2\right)^2\left\{\pi^2 + a^2 + H_t\left(1 + \gamma\right)\right\}}{a^2\left(\pi^2 + a^2 + \gamma H_t\right)} \frac{\left(\pi^2 + M_3 a^2\right)}{M_3 a^2}. \tag{33}$$

In addition, when $M_3 \to \infty$, we note that Eq. 33 turns out to be same as Eq. 27 (i.e., $R_m = R$). Equation 33 attains its critical value at $a^2 = a_c^2$, where a_c^2 satisfies the equation

$$c_1\left(a_c^2\right)^5 + c_2\left(a_c^2\right)^4 + c_3\left(a_c^2\right)^3 + c_4\left(a_c^2\right)^2 + c_5\left(a_c^2\right) + c_6 = 0, \tag{34}$$

where

$$
\begin{aligned}
c_1 &= -2M_3\\
c_2 &= -4M_3\left(\pi^2 + H_t\gamma\right)\\
c_3 &= 2\left(2\pi^4 - H_t^2M_3\gamma - H_t^2M_3\gamma^2 + H_t\pi^2 + H_t\pi^2M_3 - 2H_t\pi^2M_3\gamma\right)\\
c_4 &= 4\pi^4\left\{3\pi^2 + M_3\pi^2 + H_t\left(2+M_3\right)\left(1+\gamma\right)\right\}\\
c_5 &= 2\pi^4\left\{\pi^4\left(6+M_3\right) + H_t^2\gamma\left(2+M_3\right)\left(1+\gamma\right) + H_t\pi^2\left(5+M+8\gamma+2M_3\gamma\right)\right\}\\
c_6 &= 4\pi^6\left\{\pi^4 + H_t^2\gamma\left(1+\gamma\right) + H_t\pi^2\left(1+2\gamma\right)\right\}.
\end{aligned}
$$

4 Asymptotic Analysis for Small and Large Values of H_t

For small values of scaled heat transfer coefficient H_t, it is noted that there is almost no transfer of heat between the fluid and solid phases. The solid phase ceases to affect the thermal field of the fluid, which is free to act independently. On the other hand, for large H_t, the solid and fluid phases will have nearly identical temperatures and may be treated as a single phase. The respective mathematical problems are identical except the rescaling of R. In what follows, the expressions for the Rayleigh number R and the corresponding wave number for small as well as large values of H_t are obtained.

4.1 Case 1: $H_t \ll 1$

For this case, the Rayleigh number R is slightly above the corresponding value for the LTE case. Accordingly, we expand R given by Eq. 25 in a power series in H_t as

$$
R = \frac{\left(\pi^2+a^2\right)^2\left(\pi^2+M_3a^2\right)}{a^2\left\{\pi^2+M_3\left(1+M_1\right)a^2\right\}}\left[1 + \frac{H_t}{\left(\pi^2+a^2\right)} - \frac{\gamma H_t^2}{\left(\pi^2+a^2\right)^2} + \cdots\right]. \tag{35}
$$

In order to minimize R up to $O(H_t^2)$, we set $\partial R/\partial a = 0$ and obtain an expression of the form

$$
\begin{aligned}
&\left\{4a^2\left(1+M_1\right)M_3\pi^6 + \pi^8 + 2a^4\left(M_3^2 - 1 + 2M_1M_3 + M_1M_3^2\right)\pi^4 - 2a^8\left(1+M_1\right)M_3^2\right.\\
&\left.-2a^6M_3\pi^2\right\} + 2\pi^2\left\{a^4M_3\left(M_1+M_3+M_1M_3\right) + 2a^2\left(1+M_1\right)M_3\pi^2 + \pi^4\right\}H_t\\
&-\left\{2a^4\left(1+M_1\right)M_3^2 + 4a^2\left(1+M_1\right)M_3\pi^2 + 2\pi^4\right\}\gamma H_t^2 + \cdots = 0.
\end{aligned} \tag{36}
$$

We also expand a in power series of H_t as

$$
a = a_0 + a_1H_t + a_2H_t^2 + \cdots, \tag{37}
$$

where a_0 is the critical wave number for the LTE case and has to be obtained by solving Eq. 31 for different values of M_1 and M_3. Substituting Eq. 37 into Eq. 35 and equating the coefficients of like powers of H_t, we find a_1 and a_2 and are given by

$$
a_1 = \frac{\Delta_1}{\Delta}, \tag{38}
$$

$$
a_2 = \frac{\Delta_2}{\Delta}, \tag{39}
$$

where

$$\Delta = 8a_0 (1 + M_1) M_3\pi^6 + 8a_0^3 \left(M_3^2 + 2M_1M_3 + M_1M_3^2 - 1\right)\pi^4$$
$$-24a_0^5M_3\pi^2 - 16a_0^7 (1 + M_1) M_3^2$$
$$\Delta_1 = -\left\{2a_0^4M_3 (M_1 + M_3 + M_1M_3)\pi^2 + 4a_0^2 (1 + M_1) M_3\pi^4 + 2\pi^6\right\}$$
$$\Delta_2 = 56a_0^6a_1^2 (1 + M_1) M_3^2 - 8a_0^3a_1M_3 (M_1 + M_3 + M_1M_3)\pi^2 - 8a_0a_1 (1 + M_1) M_3\pi^4$$
$$-4a_1^2 (1 + M_1) M_3\pi^6 + 2\pi^4\gamma + 2a_0^4M_3 \left(30a_1^2\pi^2 + M_3\gamma + M_1M_3\gamma\right)$$
$$+a_0^2 \left\{4M_3\pi^2\gamma + 4M_1M_3\pi^2\gamma - 12a_1^2\pi^4 \left(2M_1M_3 + M_1M_3^2 + M_3^2 - 1\right)\right\}.$$

With the values of a_0, a_1, and a_2, Eq. 37 gives the critical wave number, and consequently, using this in Eq. 35, one can obtain the critical Rayleigh number for small H_t.

4.2 Case 2: $H_t \gg 1$

For this case, the Rayleigh number takes the form

$$R = \frac{\left(\pi^2 + M_3a^2\right)}{\left\{\pi^2 + M_3 (1 + M_1) a^2\right\}} \frac{\left(\pi^2 + a^2\right)^2}{a^2} \left(\frac{1+\gamma}{\gamma}\right) \times \left[1 - \frac{\left(\pi^2 + a^2\right)}{\gamma (1 + \gamma) H_\mathrm{t}} + \frac{\left(\pi^2 + a^2\right)^2}{\gamma^2 (1 + \gamma) H_\mathrm{t}^2} + \cdots\right]. \tag{40}$$

We minimize this with respect to a in a similar way as we did in the small H_t case and obtain the following expression:

$$2\left(a^2 + \pi^2\right)\left[M_3^2 \left(a^6 + M_1 - a^4\pi^2 (1 + M_1)\right) + M_3 \left(2a^4\pi^2 + a^2 - 2\pi^4 (1 + M_1)\right) - \pi^6\right]\gamma^2 (1 + \gamma)$$
$$+\frac{2\gamma \left(a^2 + \pi^2\right)^2}{H_\mathrm{t}} \left\{2a^6M_3^2 (1 + M_1) + a^4M_3 (4 + M_1 - M_3 (1 + M_1))\pi^2 -2a^2 (M_3 (1 + M_1) - 1)\pi^4 - \pi^6\right\} - \frac{2\left(a^2 + \pi^2\right)^3}{H_\mathrm{t}^2} \left\{3a^6 (1 + M_1) M_3^2 -a^4M_3 (-6 - 2M_1 + M_1M_3)\pi^2 + a^2 (3 - 2M_3 - M_1M_3)\pi^4 - \pi^6\right\}$$
$$+\cdots = 0. \tag{41}$$

Similarly, we expand a in the form

$$a = a_0 + \frac{a_1'}{H_\mathrm{t}} + \frac{a_2'}{H_\mathrm{t}^2} + \cdots, \tag{42}$$

where a_0 is the critical wave number for the LTE case and a_1', a_2' are to be determined. Substituting Eq. 42 into Eq. 41 and equating the coefficients of like powers of H_t, we find a_1', a_2' and are given by

$$a_1' = \frac{\Delta_1'}{\Delta'}, \tag{43a}$$

$$a_2' = \frac{\Delta_2'}{\Delta'}, \tag{43b}$$

where

$$\Delta' = -16a_0^7 (1+M_1) M_3^2\gamma^2 (1+\gamma) - 24a_0^5 M_3\pi^2\gamma^2 (1+\gamma) + 8a_0^3 \left(M_3^2 - 1 + 2M_1M_3 + M_1M_3^2\right)\pi^4\gamma^2 (1+\gamma) + 8a_0M_3 (1+M_1)\pi^6\gamma^2 (1+\gamma)$$

$$\Delta_1' = -4a_0^{10} (1+M_1) M_3^2\gamma - 2a_0^8 M_3 (4+M_1+3M_3+3M_1M_3)\pi^2\gamma^2 - 4a_0^6 (1+3M_3)\pi^4\gamma + 2a_0^4 \left(M_3^2 - 3 + 3M_1M_3 + M_1M_3^2\right)\pi^6\gamma + 4a_0^2 M_3 (1+M_1)\pi^8\gamma + 2\pi^{10}\gamma$$

$$\begin{aligned}\Delta_2' = {} & 6a_0^{12} (1+M_1) M_3^2 + 4a_0^{10} M_3 (3+M_1+4M_3+4M_1M_3)\pi^2 \\ & - 40a_0^9 a_1 (1+M_1) M_3^2\gamma + 2a_0^8 \left(3 + 16M_3 + 4M_1M_3 + 6M_3^2 + 6M_1M_3^2\right)\pi^4 \\ & - 16a_0^7 a_1 M_3 (M_1 + 4 + 3M_3 + 3M_1M_3)\pi^2\gamma - 24a_0^5 a_1 (1+3M_3)\pi^4\gamma \\ & + 8a_0^3 a_1 \left(M_3^2 - 3 + 3M_1M_3 + M_1M_3^2\right)\pi^6\gamma + 8a_0a_1M_3 (1+M_1)\pi^8\gamma \\ & - 2\pi^6 \left(2a_1^2\gamma^2 (1+\gamma) M_3 (1+M_1) + \pi^6\right) \\ & - 2a_0^4\pi^2 \left(4\pi^6M_1M_3 + \pi^6M_1M_3^2 + \pi^6M_3^2 - 6\pi^6 - 30a_1^2M_3\gamma^2 (1+\gamma)\right). \\ & + 8a_0^6 \left(2\pi^6 + 3\pi^6M_3 + 7a_1^2M_3^2\gamma^2 (1+\gamma)(1+M_1)\right) \\ & + 2a_0^2\pi^4 \begin{pmatrix} 6a_1^2\gamma^2 (1+\gamma) - 6a_1^2\gamma^2M_3^2 (1+M_1)(1+\gamma) \\ -2M_3 \left((1+M_1)\pi^6 + 6a_1^2\gamma^2 (1+\gamma) M_1\right) \end{pmatrix}.\end{aligned}$$

Again with the values of a_0, a_1', and a_2', we compute the critical wave number a_c from Eq. 42 and finally using this value of a_c, one can obtain the critical Rayleigh number R_c from Eq. 40 for large H_t. When $M_3 = 0$, it is seen that

$$a_0 = \pi, \quad a_1 = \frac{1}{4\pi}, \quad a_2 = \frac{(8\gamma+3)}{32\pi^3}, \quad a_1' = \frac{\pi^3}{\gamma(1+\gamma)}, \quad a_2' = \frac{\pi^5}{\gamma^2(1+\gamma)^2}\left(\frac{1-8\gamma}{2}\right). \tag{44}$$

The above values are the same as those obtained by Banu and Rees (2002) for an ordinary viscous fluid case.

5 Numerical Results and Discussion

The effect of LTNE on the criterion for the onset of thermomagnetic convection in a layer of ferromagnetic fluid-saturated porous medium is investigated theoretically in the presence of a uniform vertical magnetic field. Figures 2, 3, and 4 give the neutral curves (R against a) for different values of γ (with $M_1 = 1 = M_3$), M_1 (with $\gamma = 0.5$, $M_3 = 1$), and M_3 (with $\gamma = 0.5$, $M_1 = 1$), respectively, when $H_t = 100$. The neutral curves exhibit single but different, minimum with respect to the wave number, and their shape is identical in the form to that of the Darcy–Benard problem. For increasing values of γ (see Fig. 2) and M_3 (see Fig. 4), the neutral curves are skewed toward the lower wave number region, while for increasing values of M_1 (see Fig. 3) they are tilted toward higher wave number region. In general, R decreases with the increase in the value of γ, M_1, and M_3. Large values of γ amounts to heat transported through both the solid and fluid phases, whereas small values correspond to heat transport primarily through the fluid phase. Therefore, convection is established quickly at higher values of γ when other parameters are held fixed. The size of M_1 is related to the importance of magnetic forces as compared to gravitational forces. The case $M_1 = 0$ corresponds to convective instability in an ordinary viscous fluid saturating a porous medium

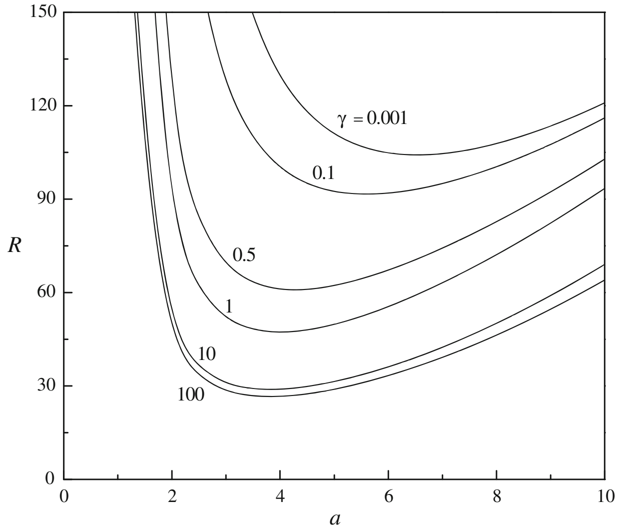

Fig. 2 Neutral curves for different values of γ with $M_1 = 1$, $M_3 = 1$ and $H_t = 100$

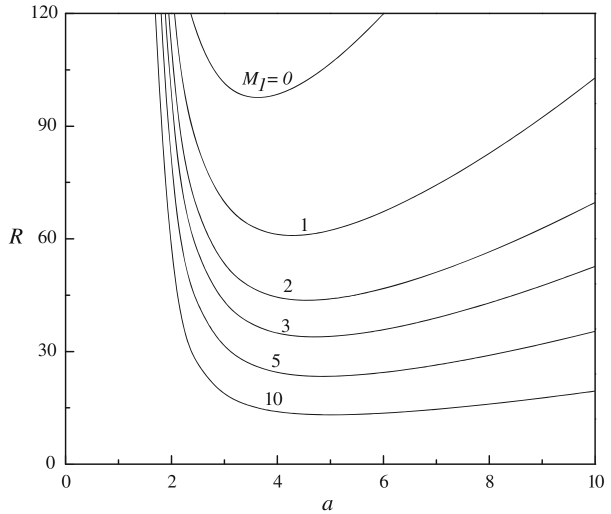

Fig. 3 Neutral curves for different values of M_1 with $\gamma = 0.5$, $M_3 = 1$ and $H_t = 100$

and in that case only the buoyancy forces contribute to the instability. From Fig. 3, it is seen that an increase in M_1 leads to decrease in the critical Rayleigh number and thus makes the system more unstable. This is due to an increase in the destabilizing magnetic force with increasing M_1, which favors the fluid to flow more easily. In other words, the magnetic fluid carries heat more efficiently than the ordinary viscous fluid. Similarly, increase in the value of M_3 makes the ferrofluid to acquire larger magnetization which in turn interacts with the imposed magnetic field and releases more energy to drive the flow faster. Hence, the system becomes unstable with a smaller temperature gradient (i.e., at smaller Rayleigh number) as the value of M_3 increases. Alternatively, a higher value of M_3 would arise either due to a

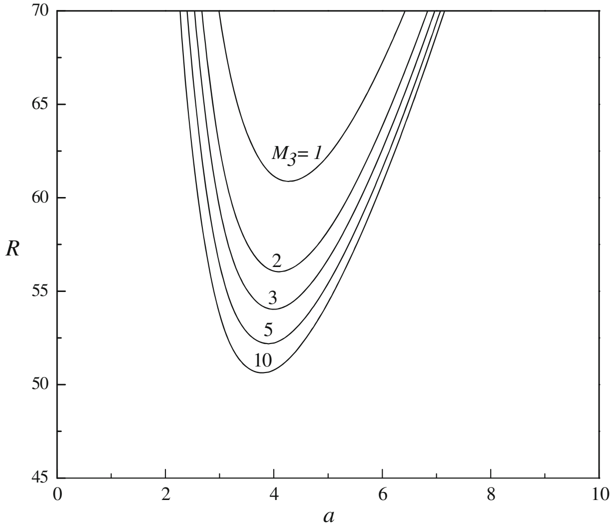

Fig. 4 Neutral curves for different values of M_3 with $\gamma = 0.5$, $M_1 = 1$ and $H_t = 100$

larger pyromagnetic coefficient or larger temperature gradient. Both these factors are conducive for generating a larger gradient in the Kelvin body force field, possibly promoting the instability.

In order to determine the criterion for the onset of convection, the critical Darcy–Rayleigh number R_c obtained with respect to the wave number a is the important value. Hence, the behavior of R_c has been summarized in Figs. 5a, 6a and 7a as a function of $\log_{10} H_t$ for different values of γ (with $M_1 = 1 = M_3$), M_1 (with $\gamma = 0.5, M_3 = 1$), and M_3 (with $\gamma = 0.5, M_1 = 1$), respectively. The corresponding critical wave numbers a_c are shown in Figs. 5b, 6b and 7b. We note that the curves of different γ coalesce and asymptote to a single R_c value when H_t is small and the critical Darcy–Rayleigh number remains almost independent of H_t for $\gamma \geq 10$ (see Fig. 5a). This is because, for very small values of H_t and higher values of γ there is no significant transfer of heat between the fluid and solid phases, and hence the condition for the onset of convection is not affected by the properties of the solid phase. This corresponds to classical LTE limit. However, R_c varies with γ as the value of H_t goes on increasing and remains independent of H_t at higher values of H_t. The figure also indicates that for moderate and large values of H_t, the critical Darcy–Rayleigh number decreases with the increasing values of γ. In other words, increasing γ is to hasten the onset of thermomagnetic convection because heat is transported to the system through both by solid and fluid phases. A similar trend could be seen with increasing M_1 (see Fig. 6a) and M_3 (see Fig. 7a), but for small values of H_t the curves of different M_1 and M_3 do not coalesce. We again see the fact that an increase in the value of M_1 and M_3 is to hasten the onset of thermomagnetic convection (i.e., to decrease the critical Darcy–Rayleigh number).

The critical wave number remains the same for different values of γ in both the small and large H_t limits and this is evident from Fig. 5b. However, at moderate values of H_t, the critical wave number reaches its peak value and increasing γ decreases the value of a_c. In other words, increase in the value of γ is to enlarge the size of convection cells only at moderate values of H_t and the size of convection cells remains independent of γ when $H_t \ll 1$ and $H_t \gg 1$. Although the critical wave number remains the same when $H_t \ll 1$ and $H_t \gg 1$ for

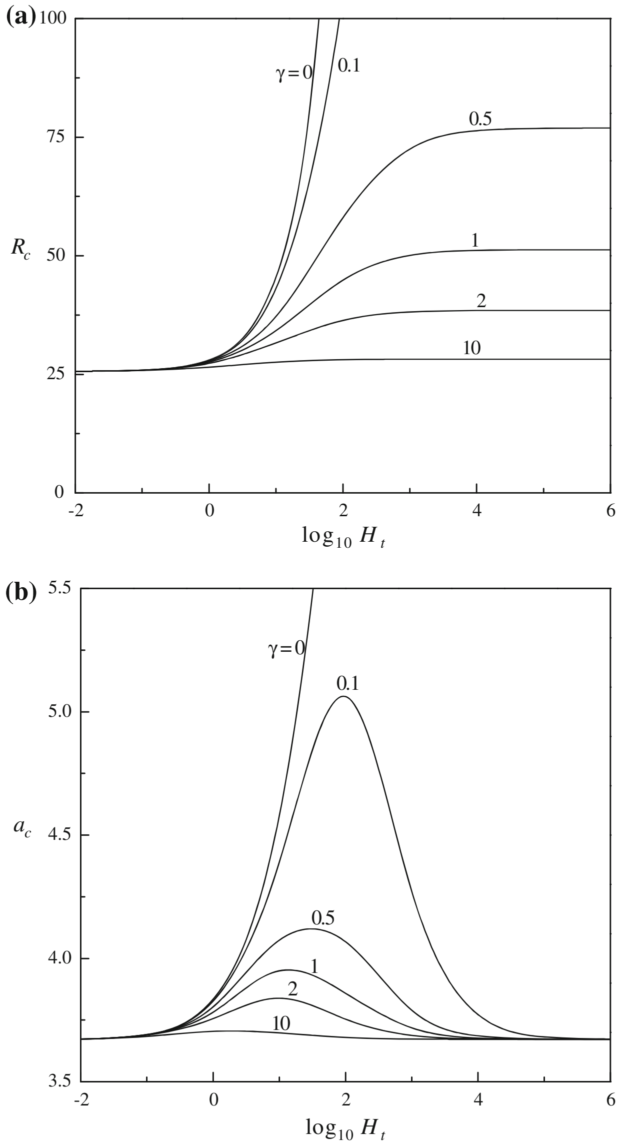

Fig. 5 **a** Variation of R_c with $\log_{10} H_t$ for different values of γ with $M_1 = 1$ and $M_3 = 1$. **b** Variation of a_c with $\log_{10} H_t$ for different values of γ with $M_1 = 1$ and $M_3 = 1$

a fixed value of M_1 (Fig. 6b) as well as M_3 (Fig. 7b), the curves of a_c for different M_1 and M_3 do not join together under these two limiting cases of H_t. We note that increasing M_1 is to increase the critical wave number, while opposite is the case with increasing M_3. That is, increase in the value of M_1 and decrease in M_3 is to diminish the size of convection cells for all values of H_t.

The critical value of R_m obtained with respect to the wave number is denoted by R_{mc} and the corresponding critical wave number is denoted by a_{mc}. In Fig. 8a, the variations of

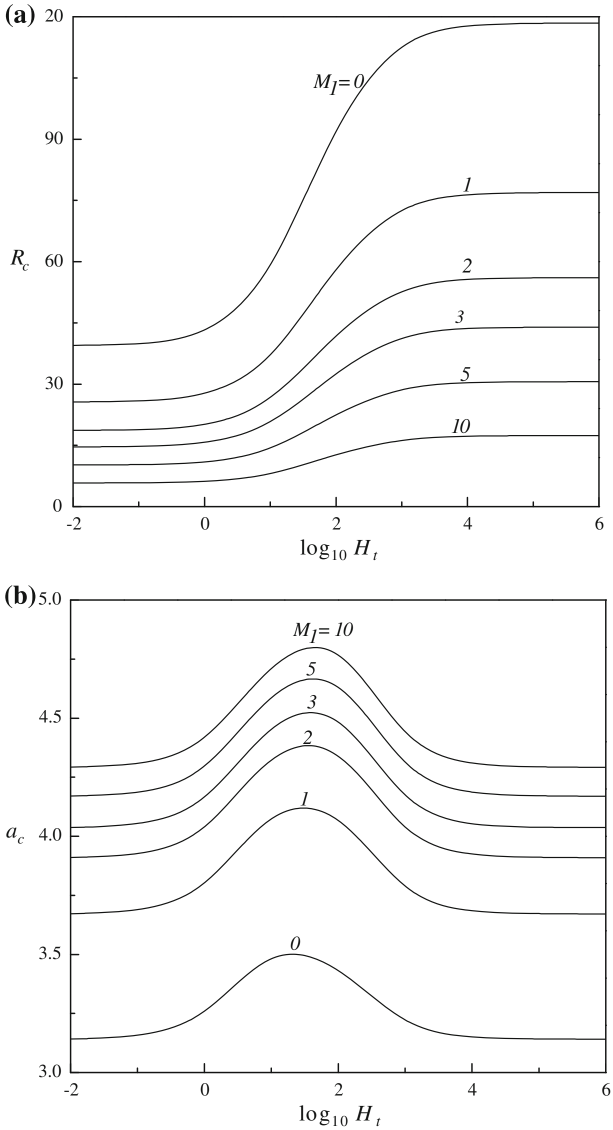

Fig. 6 **a** Variation of R_c with $\log_{10} H_t$ for different values of M_1 with $\gamma = 0.5$ and $M_3 = 1$. **b** Variation of a_c with $\log_{10} H_t$ for different values of M_1 with $\gamma = 0.5$ and $M_3 = 1$

R_{mc} and R_c as a function of $\log_{10} H_t$ are presented for two values of γ and M_3 to assess the impact of magnetic forces alone and the combined effect of magnetic and buoyancy forces on the onset of thermomagnetic convection. From the figure, it is seen that $R_{mc} < R_c$ always, and hence the system is more stabilizing when the magnetic forces alone are present (i.e., in the absence of buoyancy forces). Similar is the case with the critical wave number (Fig. 8b). From the figures, it is also observed that the effect of γ and M_3 on R_{mc} and a_{mc} is more pronounced than on R_c and a_c.

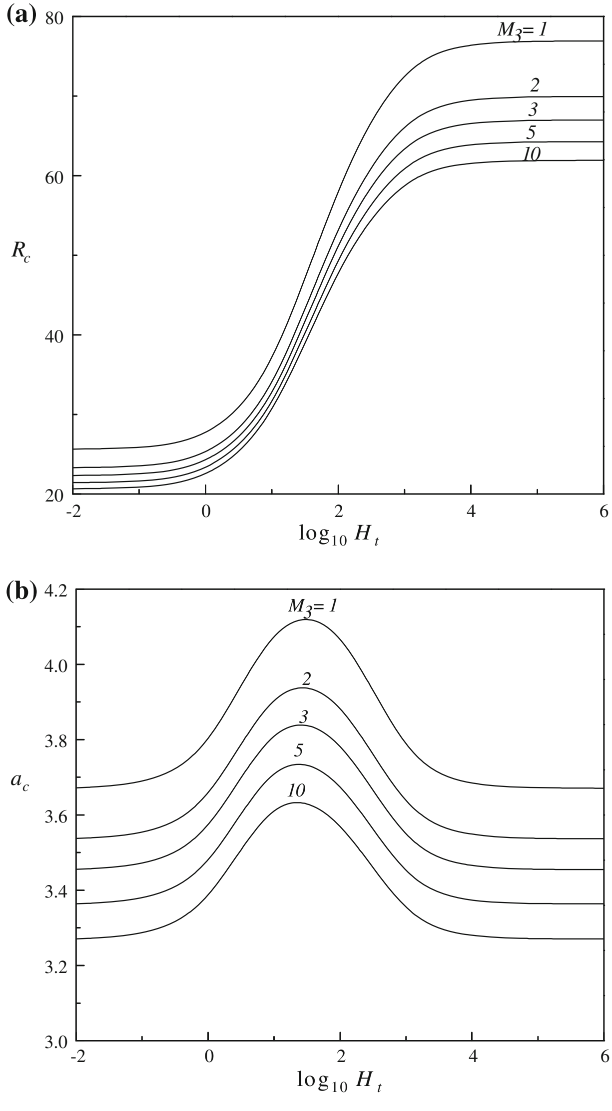

Fig. 7 **a** Variation of R_c with $\log_{10} H_t$ for different values of M_3 with $\gamma = 0.5$ and $M_1 = 1$. **b** Variation of a_c with $\log_{10} H_t$ for different values of M_3 with $\gamma = 0.5$ and $M_1 = 1$

The critical Darcy–Rayleigh number, R_c, and the corresponding critical wave number, a_c, are obtained for both small as well as large H_t using the asymptotic formulae (cf. Eqs. 35, 37, 40, and 42). The critical stability parameters (R_c, a_c) so obtained are compared with the exact values obtained from Eq. 25 in Tables 1 and 2 for representative values of $M_1 = 1 = M_3$ with $\gamma = 1$ and $M_1 = 5 \quad M_3 = 1$ with $\gamma = 1$, respectively. From the tables, it is observed that an increasingly good agreement among the critical stability parameters as the value of H_t either decreases or increases.

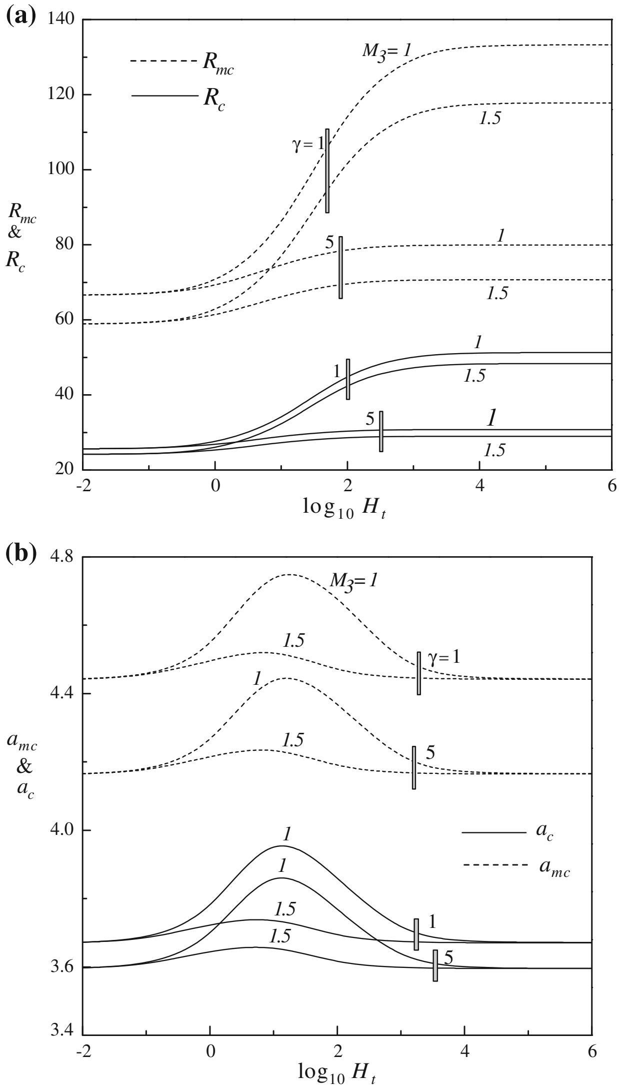

Fig. 8 **a** Variation of R_c and R_{mc} with $\log_{10} H_t$ for different values of γ and M_3. **b** Variation of a_c with $\log_{10} H_t$ for different values of γ and M_3

6 Conclusions

The onset of thermomagnetic convection in a horizontal layer of ferromagnetic fluid-saturated porous medium heated from below is examined analytically in the presence of a uniform magnetic field when the temperature of the solid and fluid phases are not in local thermal equilibrium. The results of the foregoing study can be summarized as follows:

(i) The neutral stability curves for various values of physical parameters exhibit that the onset of thermomagnetic convection retains its unimodal shape with one distinct

Table 1 Comparison of the asymptotic (A) and exact (E) values of the critical Darcy–Rayleigh number (R_c) and the critical wave number (a_c) for different values of H_t with $M_1 = 1 = M_3$ and $\gamma = 1$

$\log_{10} H_t$	$R_c(A)$	$a_c(A)$	$R_c(E)$	$a_c(E)$
−2.0	25.6530	3.67265	25.6530	3.67265
−1.0	25.7512	3.6817	25.7512	3.68017
0.0	26.6813	3.74607	26.6831	3.74176
1.0	32.1051	3.476	33.0471	4.02396
2.0	46.6299	3.85876	46.3171	3.8588
3.0	50.6971	3.69446	50.6968	3.69445
4.0	51.2242	3.67411	51.2242	3.67411
5.0	51.2780	3.67203	51.2780	3.67203

Table 2 Comparison of the asymptotic (A) and exact (E) values of the critical Darcy–Rayleigh number (R_c) and the critical wave number (a_c) for different values of H_t with $M_1 = 5$, $M_3 = 1$ and $\gamma = 1$

$\log_{10} H_t$	$R_c(A)$	$a_c(A)$	$R_c(E)$	$a_c(E)$
−2.0	10.2027	4.17012	10.2027	4.17012
−1.0	10.2362	4.17719	10.2362	4.17719
0.0	10.5557	4.24027	10.5562	4.24107
1.0	12.5881	4.11245	12.8307	4.53349
2.0	18.353	4.40028	18.1551	4.40006
3.0	20.1264	4.19819	20.1262	4.19819
4.0	20.3702	4.17227	20.3702	4.17227
5.0	20.3952	4.16962	20.3952	4.16962

minimum which defines the critical Darcy–Rayleigh number and the corresponding wave number.

(ii) The porosity modified conductivity ratio γ has no effect on the onset of thermomagnetic convection in the small-H_t limit, while for the other values of H_t increase in the value of γ is to hasten the onset of convection. At higher values of γ, the onset of convection remains independent of H_t and tends to classical LTE case.

(iii) The effect of increase in the magnetic number M_1 and the nonlinearity of magnetization parameter M_3 are to advance the onset of thermomagnetic convection.

(iv) The system is more stabilizing when the magnetic forces alone are present, and in that case M_3 and γ show prominence effect on the onset of convection when compared to the simultaneous presence of buoyancy and magnetic forces.

(v) The critical wave number for different values of γ in the small-H_t and large-H_t limits coincide, but attain a maximum value at the intermediate values of H_t and in that case increasing γ decreases the critical wave number.

(vi) For different values of M_1 and M_3, the critical wave number remains the same when $H_t \ll 1$ and $H_t \gg 1$ but for the intermediate values it attains the maximum, which is always greater than the LTE case. Increase in the value of M_1 is to increase the critical wave number but opposite is the case with increasing M_3.

Acknowledgements One of the authors (ISS) wishes to thank the BK21 Program of the School of Mechanical Engineering, Yonsei University, Seoul, Korea, for inviting him as a visiting Professor and also the Bangalore University for sanctioning sabbatical leave.

References

Alexiou, C., Arnold, W., Hulin, P., Klein, R., Schmidt, A., Bergemann, C., Parak, F.G.: Therapeutic efficacy of ferrofluid bound anticancer agent. Magnetohydrodynamics **37**, 318–322 (2001)

Banu, N., Rees, D.A.S.: Onset of Darcy–Benard convection using a thermal non-equilibrium model. Int. J. Heat Mass Transf. **45**, 2221–2228 (2002)

Berkovsky, B.M., Medvedev, V.F., Krakov, M.S.: Magnetic Fluids, Engineering Applications. Oxford University Press, New York (1993)

Blums, E., Cebers, A., Maiorov, M.M.: Magnetic Fluids. de Gruyter, New York (1997)

Borglin, S.E., Mordis, J., Oldenburg, C.M.: Experimental studies of the flow of ferrofluid in porous media. Transp. Porous Med. **41**, 61–80 (2000)

Finlayson, B.A.: Convective instability of ferromagnetic fluids. J. Fluid Mech. **40**, 753–767 (1970)

Hergt, R., Andrä, W., Ambly, C.G., Hilger, I., Kaiser, W.A., Richter, U., Schmidt, H.G.: Physical limitations of hypothermia using magnetite fine particles. IEEE Trans. Magn. **34**, 3745–3754 (1998)

Kuznetsov, A.V.: Thermal non-equilibrium forced convection in porous media. In: Ingham, D.B., Pop, I. (eds.) Transport Phenomena in Porous Media, pp. 103–130. Pergamon, Oxford (1998)

Malashetty, M.S., Shivakumara, I.S., Sridhar, K.: The onset of Lapwood–Brinkman convection using a thermal non-equilibrium model. Int. J. Heat Mass Transf. **48**, 1155–1163 (2005a)

Malashetty, M.S., Shivakumara, I.S., Sridhar, K.: The onset of convection in an anisotropic porous layer using a thermal non-equilibrium model. Transp. Porous Med. **60**, 199–215 (2005b)

Malashetty, M.S., Shivakumara, I.S., Sridhar, K., Mahantesh, S.: Convective instability of Oldroyd-B fluid saturated porous layer heated from below using a thermal non-equilibrium model. Transp. Porous Med. **64**, 123–139 (2006)

Matura, P., Lucke, M.: Thermomagnetic convection in a ferrofluid layer exposed to a time-periodic magnetic field. Phys. Rev. E **80**, 026314–026322 (2009)

Nanjundappa, C.E., Shivakumara, I.S.: Effect of velocity and temperature boundary conditions on convective instability in a ferrofluid layer. ASME J. Heat Transf. **130**, 104502-1–104502-5 (2008)

Nanjundappa, C.E., Shivakumara, I.S., Arunkumar, C.: Benard–Marangoni ferroconvection with magnetic field dependent viscosity. J. Magn. Magn. Mat **322**, 2256–2263 (2010)

Nield, D.A., Bejan, A.: Convection in Porous Media, 3rd edn. Springer, New York (2006)

Nouri-Borujerdi, A., Noghrehabadi, A.R., Rees, D.A.S.: Onset of convection in a horizontal porous channel with uniform heat generation using a thermal non-equilibrium model. Transp. Porous Med. **69**, 343–357 (2007a)

Nouri-Borujerdi, A., Noghrehabadi, A.R., Rees, D.A.S.: The effect of local thermal non-equilibrium on impulsive conduction in porous media. Int. J. Heat Mass Transf. **50**, 3244–3249 (2007b)

Odenbach, S.: Recent progress in magnetic fluid research. J. Phys. Condens. Mat. **16**, R1135–R1150 (2004)

Postelnicu, A., Rees, D.A.S.: The onset of Darcy–Brinkman convection in a porous medium using a thermal non-equilibrium model. Part I: stress-free boundaries. Int. J. Energy Res. **27**, 961–973 (2003)

Postelnicu, A.: The onset of a Darcy–Brinkman convection using a thermal non-equilibrium model. Part II. Int. J. Therm. Sci. **47**, 1587–1594 (2008)

Qin, Y., Chadam, J.: A non-linear stability problem for ferromagnetic fluids in a porous medium. Appl. Math. Lett. **8**(2), 25–29 (1995)

Rees, D.A.S., Pop, I.: Free convective stagnation-point flow in a porous medium using a thermal non-equilibrium model. Int. Commun. Heat Mass Transf. **26**, 945–954 (1999)

Rees, D.A.S., Pop, I.: Vertical free convective boundary layer flow in a porous medium using a thermal non-equilibrium model. J. Porous Med. **3**, 31–44 (2000)

Rees, D.A.S., Pop, I.: Vertical free convective boundary-layer flow in a porous medium using a thermal non-equilibrium model: elliptic effects. J. Appl. Math. Phys. (ZAMP) **53**, 1–12 (2002)

Rees, D.A.S., Pop, I. : Local thermal non-equilibrium in porous medium convection. In: Ingham, D.B., Pop, I. (eds.) Transport Phenomena in Porous Media, vol. III, pp. 147–173. Elsevier, Oxford (2005)

Rosensweig, R.E.: Ferrohydrodynamics. Cambridge University Press, Cambridge, London (1985)

Rosensweig, R.E., Zahn, M., Volger, T. : Stabilization of fluid penetration through a porous medium using magnetizable fluids. In: Berkovsky, B. (ed.) Thermomechanics of magnetic fluids, pp. 195–211. Hemisphere, Washington, DC (1978)

Shivakumara, I.S., Malashetty, M.S., Chavaraddi, K.B.: Onset of convection in a viscoelastic fluid-saturated sparsely packed porous layer using a thermal non-equilibrium model. Can. J. Phys. **84**, 973–990 (2006)

Shivakumara, I.S., Nanjundappa, C.E., Ravisha, M.: Thermomagnetic convection in a magnetic nanofluids fluid saturated porous medium. Int. J. Appl. Math. Eng. Sci. **2**(2), 157–170 (2008)

Shivakumara, I.S., Nanjundappa, C.E., Ravisha, M.: Effect of boundary conditions on the onset of thermomagnetic convection in a ferrofluid saturated porous medium. ASME J. Heat Transf. **131**, 101003-1-9 (2009)

Shivakumara, I.S., Mamatha, A.L., Ravisha, M.: Effects of variable viscosity and density maximum on the onset of Darcy–Benard convection using a thermal non-equilibrium model. J. Porous Med. (2010a). (to appear)

Shivakumara, I.S., Mamatha, A.L., Ravisha, M.: Boundary and thermal non-equilibrium effects on the onset of Darcy–Brinkman convection in a porous layer. J. Eng. Math. (2010b). doi:10.1007/s10665-010-9362-3

Singh, J., Bajaj, R.: Temperature modulation in ferrofluid convection. Phys. Fluids **21**, 064105-1–064105-12 (2009)

Straughan, B.: Global nonlinear stability in porous convection with a thermal non-equilibrium model. Proc. R. Soc A **462**, 409–418 (2006)

Sunil, Mahajan, A.: A non-linear stability analysis for magnetized ferrofluid heated from below. Proc. R. Soc. Lond. A **464**, 88–94 (2008)

Sunil, Mahajan, A.: Nonlinear stability analysis for thermoconvective magnetized ferrofluid saturating a porous medium. Transp. Porous Med. **76**, 327–343 (2009)

Vafai, K., Amiri, A.: Non-Darcian effects in combined forced convective flows. In: Ingham, D.B., Pop, I. (eds.) Transport Phenomena in Porous Media, pp. 313–329. Pergamon, Oxford (1998)

Vaidaynathan, G., Sekar, R., Balasubramanian, R.: Ferroconvective instability of fluids saturating a porous medium. Int. J. Eng. Sci. **29**, 1259–1267 (1991)

Zhan, M., Rosensweig, R.E.: Stability of magnetic fluid penetration through a porous medium with uniform magnetic field oblique to the interface. IEEE Trans. Magn. **16**, 275–282 (1980)